Metrol. Meas. Syst., Vol. 30 (2023) No. 1, pp. 99–115
DOI: 10.24425/mms.2023.144396

PAN POLSKA AKADEMIA NAUK

METROLOGY AND MEASUREMENT SYSTEMS
Index 330930, ISSN 0860-8229
www.metrology.wat.edu.pl

M&MS

PARAMETER IDENTIFICATION APPROACH USING IMPROVED TEACHING AND LEARNING BASED OPTIMIZATION FOR HUB MOTOR CONSIDERING TEMPERATURE RISE

Yong Li[1)], Juan Wang[2)], Taohua Zhang[2)], Han Hu[1)], Hao Wu[1)]

1) Automotive Engineering Research Institute, Jiangsu University, Zhenjiang 212013, China
(✉ *liyongthinkpad@outlook.com*, *huhanxx20@163.com*, *wu5hao@foxmail.com*)
2) Beijing Institute of Space Launch Technology, Beijing 100076, China
(*wangjuan1104@126.com*, *641106388@qq.com*)

Abstract

Temperature rise of the hub motor in *distributed drive electric vehicles* (DDEVs) under long-time and overload operating conditions brings parameter drift and degrades the performance of the motor. A novel online parameter identification method based on *improved teaching-learning-based optimization* (ITLBO) is proposed to estimate the stator resistance, d-axis inductance, q-axis inductance, and flux linkage of the hub motor with respect to temperature rise. The effect of temperature rise on the stator resistance, d-axis inductance, q-axis inductance, and magnetic flux linkage is analysed. The hub motor parameters are identified offline. The proposed ITLBO algorithm is introduced to estimate the parameters online. The Gaussian perturbation function is employed to optimize the TLBO algorithm and improve the identification speed and accuracy. The mechanisms of group learning and low-ranking elimination are established. After that, the proposed ITLBO algorithm for parameter identification is employed to identify the hub motor parameters online on the test bench. Compared with other parameter identification algorithms, both simulation and experimental results show the proposed ITLBO algorithm has rapid convergence and a higher convergence precision, by which the robustness of the algorithm is effectively verified.

Keywords: parameters identification, teaching–learning-based optimization, hub motor, temperature rise.

1. Introduction

With the development of *electric vehicle* (EV) technologies, the distributed in-wheel motor drive EV has attracted many scholars' attention due to the advantages of optimized structure, high efficiency, and strong manoeuvrability [1]. The hub motor is the core component of the drive system. Restricted by the working environment, operating conditions, and economy, the motor drive system is supposed to have a fast response, high power density, high reliability, and low cost [2, 3].

Article history: received September 11, 2022; revised October 28, 2022; accepted October 28, 2022; available online January 19, 2023.

The hub motor drive system consists of a hub motor and controller, which are highly integrated and installed inside the narrow wheel hub. Generally, motor speed is detected by traditional hall sensors or a resolver installed on the stator of the motor [4, 5]. However, the hall sensor or resolver can be easily and seriously affected by the road impact, vibration, motor thermal energy, and inverter dead zone, which brings poor sensitivity and temperature drift [6]. Moreover, the position sensor also increases the complexity of motor structure, system cost, and maintenance difficulty. A rotor position detection technology, which is also called sensorless control, provides an effective solution to solve the problems. The sensorless control technology is supposed to realize the detection of the rotor position and speed, by using the rich information resources of voltage and current of the hub motor drive system [7–10].

Sensorless control is helpful to further improve the integration level of the hub motor. However, the sensorless control strategy, especially at a low speed, mainly depends on the motor model and key parameters such as stator resistance, *dq*-axis inductances, and flux linkage [11–13]. Accurate identification of motor parameters is the basis for sensorless control. Moreover, considering the system safety, the motor parameters can also provide support for current vector control to obtain high dynamic and static performance for the hub motor [14–16]. The above-mentioned motor parameters mainly depend on the temperature rise, magnetic saturation, *voltage-source inverter* (VSI) nonlinearities, and load disturbance under different operating conditions. Parameter variation will lead to a change in the system operational state of the hub motor drive system [17]. Therefore, it is necessary to obtain the accurate parameters of the hub motor due to its harsh operating conditions. Reference [18] estimates the stator resistance and *dq*-axis inductances for sensorless control of *permanent magnet synchronous motors* (PMSMs). Resistance, inductance, and flux linkage of the motor are estimated in [19]. Reference [20] estimates the resistance, inductance, flux linkage considering inverter nonlinearity. Resistance, the *dq*-axis inductances, and the magnetic flux linkage are identified based on the high-frequency equivalent impedance model of the motor with high-frequency injection which is proposed in [21]. In [22], stator resistance, *dq*-axis inductances, and flux linkage are estimated based on the dynamic particle swarm optimization with a learning strategy regarding VSI nonlinearities for PMSMs. System identifiability and VSI nonlinearities are considered in [23] to identify the parameters for PMSMs.

Numerous offline and online identification methods are employed by scholars for parameter identification. Although the off-line parameter identification method provides more accurate initial parameters for a speed regulation system, the motor parameters will change nonlinearly with the motor torque, current, and the coupling of the thermal-electromagnetic field. Also, the table-checking method is employed for offline parameter identification. However, this method needs a large memory space to store offline identification data. The identification accuracy of the table-checking method is low and cannot provide accurate parameters for the hub motor drive and be effectively controlled under complex working conditions. Scholars have proposed a lot of online parameter estimation methods, including the *least square* (LS) method [24], the extended Kalman filter (EKF) method [25], the *model reference adaptive system* (MRAS) method [26], the *neural network* (NN) algorithm [27], the *genetic algorithm* (GA) [28], the *particle swarm optimization algorithm* (PSO) [29, 30], and the *artificial bee colony* (ABC) algorithm [31]. In [24], the LS method is proposed to update parameter estimation by using the modified modelling error of online historical data and instant data as additional feedback. Integral transformation is used to avoid the time deviation of the plant state in the modified modelling error. The Kalman filter theory was first proposed to solve the Gaussian white noise problem for a linear discrete dynamic system, and then extended to solve the same problem for a nonlinear system. In [25], the estimation accuracy of the traditional EKF and adaptive extended Kalman Filters are compared. In [26], the MRAS method is applied to induction motors to simultaneously detect both

Metrol. Meas. Syst., Vol. 30 (2023), No. 1, pp. 99–115
DOI: 10.24425/mms.2023.144396

the rotor position and the stator resistance. The swarm intelligence algorithm shows intelligence through cooperation among many non-intelligent individuals. In [27], the voltage equation of the surface-mount PMSM considering the voltage source nonlinearities is transformed to eliminate the influence of the error voltage. A variable step size Adaline NN algorithm is studied to estimate the parameters. In [28], the mathematical model of the motor is discretized by a Padé Approximant, and the parameters are identified by GA. In [29], aiming at the problem of low efficiency of PSO, a growth rate operator reflecting the state of particles is designed to judge the state of particles, and search efficiency is improved by the Gaussian perturbation function. In [30], a PSO-based identification method for identifying five parameters simultaneously is proposed. Two particle swarm algorithms are applied simultaneously, one particle group to estimate the motor parameters, and the other particle group to optimize the parameters of the first. In [31], the ABC algorithm is employed to identify the parameter of the interval discrete dynamic model.

The current research mainly focuses on parameter identification of magnetic saturation, voltage-source inverter nonlinearity, and load disturbance. However, a few researchers investigate the effect of temperature rise on hub motor parameters. The hub motor drive EV faces frequent start, stop, acceleration, deceleration, and overload conditions during the drive cycle, especially when it is operating in the urban area. The hub motor works under low speed and large output torque for a long time, which leads to high temperature. It is necessary to investigate the effective and accurate parameter identification method that can be applied to the temperature rise of the hub motor for *distributed drive electric vehicles* (DDEVs).

A *teaching-learning-based optimization* (TLBO) algorithm is a cluster optimization method proposed by Indian scholars R.V. Rao and V.D. Kalyankar in 2011 which simulates the teaching and learning process [32, 33]. TLBO had attracted the researchers' attention since it was proposed due to its advantages of few parameters, simple algorithm, easy understanding, rapid convergence, strong convergence ability, and high accuracy. The teaching ability of TLBO is simple, and a local optimum will easily appear for some large-scale complex problems. That, however, may affect the its global search ability and make the algorithm early fall into a local optimum, which leads to poor convergence and less population diversity. The improved teaching-learning-based optimization (ITLBO) is proposed in our work to satisfy the need to efficiently evaluate the temperature rise of the hub motor and quickly obtain accurate parameters under complex operating conditions.

The major contribution of our work is listed as follows.

1. This paper not only introduced a teaching-learning artificial intelligence optimization algorithm for the identification of motor parameters, but also improved the structure of TLBO optimization algorithm.
2. The proposed ITLBO optimization algorithm increases the speed of convergence of the identified parameters, and bench experiments verify the superiority and reliability of this algorithm.

The paper is structured as follows. Section 2 briefly introduces the hub motor mathematical model. Section 3 analyses the effect of temperature on the parameters of a hub motor. The parameter models are also established. Section 4 presents the basic principle and working process of the proposed ITLBO method for parameter identification. The *model-in the-loop* (MiL) simulation and experiment are carried out in Section 5. Section 6 shows conclusions and future work.

2. Mathematical model of the hub motor

The following assumptions are considered regarding the hub motor to ensure the research results:

1. Ignoring the saturation of the core magnetic circuit and the space harmonics.

2. Assuming that the three-phase windings are completely symmetrical.
3. Assuming that the electromotive force is a standard sine wave.

Based on the above, the voltage equation of the hub motor is described as:

$$\begin{cases} u_d = R_s i_d + p\psi_d - \omega_e \psi_q \\ u_q = R_s i_q + p\psi_q + \omega_e \psi_d \end{cases}, \tag{1}$$

where, u_d is the d-axis voltage. u_q is the q-axis voltage. i_d is the d-axis current. i_q is the q-axis current. ψ_d is the d-axis flux linkage. ψ_q is the q-axis flux linkage. p is a differential operator. R_s is the stator resistance. ω_e is the electric angular velocity.

$$\begin{cases} \psi_d = \psi_f + L_d i_d \\ \psi_q = L_q i_q \end{cases}, \tag{2}$$

where, L_d and L_q are the dq-axis inductances, respectively. ψ_f is the flux linkage.

The following equation can be obtained when combining equation (2) into equation (1):

$$\begin{cases} u_d = R_s i_d + L_d p i_d - \omega_e L_q i_q \\ u_q = R_s i_q + L_q p i_q + \omega_e L_d i_d + \omega_e \psi_f \end{cases}. \tag{3}$$

3. Off-line parameter identification analysis

The temperature of the hub motor rises inevitably under harsh working environments and high loads while the vehicle is operating on the road. Accurate motor parameters provide solid support for sensorless control [34]. However, these parameters are sensitive to temperature rise. This section presents an offline parameter identification method for hub motor and verifies the correctness of the theoretical analysis of the temperature effect on the hub motor parameters.

3.1. Effect of temperature rise on stator resistance of the hub motor

Experimental results show that the resistivity of all pure metals increases with temperature rise. The resistivity changes linearly with temperature when it is not too low. As a parameter that reflects the change of resistance with temperature, the temperature coefficient of resistance (TCR) is widely used in reliability tests of metal interconnectors. The stator winding material of the hub motor is copper, the TCR of which also changes with temperature. The TCR of copper at a temperature of t can be expressed by the following equation:

$$\alpha = \frac{1}{T + t}. \tag{4}$$

The stator resistance is described as:

$$R_t = R_0 \left[1 + \alpha (t - t_0)\right], \tag{5}$$

where R_t is the resistance changing with temperature t, R_0 is the resistance changing with temperature t_0, T is the temperature coefficient of resistance.

The resistance value of the hub motor stator winding can be measured by the DC test method. The stable current response value I_{d1} and I_{d2} can be measured after a time of t when the fixed voltage U_{d1} and U_{d2} are injected into the motor. In result, we obtain the following equation:

$$R_s = \frac{2\left(U_{d1} - U_{d2}\right)}{3\left(I_{d1} - I_{d2}\right)}. \tag{6}$$

Metrol. Meas. Syst., Vol. 30 (2023), No. 1, pp. 99–115
DOI: 10.24425/mms.2023.144396

3.2. Effect of temperature rise on dq-axis inductances of the hub motor

According to the zero-state response of the RL circuit, the d-axis current response of the hub motor will be obtained by a voltage vector injection with a constant amplitude to the d-axis of the hub motor. The d-axis current response of the motor is expressed as equation (7) and equation (8). Letting $-R_s/L_d \cdot \tau = -1$ in equation (8), the current becomes 0.632 times of the steady current at this time. The d-axis inductance can be calculated by equation (9). The q-axis inductance can be obtained by employing a short-time pulse injection. Through the tests at different temperatures, we can see that the residual magnetic field density of the permanent magnet in the rotor decreases with the temperature rise, which reduces the saturation of the rotor magnetic circuit. The dq-axis inductances of the hub motor increase with the temperature rise.

$$u_d = R_d i_d + L_d \frac{di_d}{d\tau}, \tag{7}$$

$$i(t) = \frac{u_d}{R_d}\left(1 - e^{-\frac{R_s}{L_d}\tau}\right), \tag{8}$$

$$L_d = t_{0.632} \cdot R_s\,, \tag{9}$$

where R_d is the d-axis resistance, $R_d = 2R$, R_q is the q-axis resistance, $R_q = 3/2R_s$.

3.3. Effect of temperature rise on flux linkage of the hub motor

The without-load method is generally employed for rotor flux parameter identification of the hub motor, which makes the motor work in a stable state [35]. The voltage and current of the hub motor are acquired twice to obtain the accurate value of flux value. The following equation can be obtained by coordination transformation:

$$\begin{cases} u_{q1} = R_s i_q + \omega_e L_d i_{d1} + \omega_e \psi_f \\ u_{q2} = R_s i_q + \omega_e L_d i_{d2} + \omega_e \psi_f \end{cases}. \tag{10}$$

I. The flux value can be obtained from equation (10), which can be expressed as in [36]:

$$\psi_f = \frac{u_{q1} i_{d2} - u_{q2} i_{d1}}{\omega_e (i_{d2} - i_{d1})} - \frac{R_s i_q}{\omega_e}. \tag{11}$$

II. The flux is approximately linear to temperature, which can be expressed as

$$\psi_f = at + b. \tag{12}$$

4. Online parameter identification based on the ITLBO algorithm

4.1. Basic principle of TLBO

The basic TLBO algorithm includes the concepts of class, student, and teacher. The mathematical explanation of the algorithm is described as follows:

1. Class: All the individuals in a population of class. The search space of algorithm $S = (X_1, X_2 \ldots X_N)$. N represents the population size.
2. Learner: The individual sample X in the class is called a learner, where $X = (x_1, x_2 \ldots, x_d)$. x_i is the i-th subject that learner$X$ has learned which is equivalent to a decision variable. $d$is the variable dimension.

3. Teacher: The best learner in the class is supposed to be the teacher X_t, which represents the optimal individual.

A class can be described as follows:

$$\begin{bmatrix} X_1 & | & f(X_1) \\ X_2 & | & f(X_2) \\ \vdots & | & \vdots \\ X_N & | & f(X_N) \end{bmatrix} = \begin{bmatrix} x_1^1 & x_2^1 & \cdots & x_d^1 & | & f(X_1) \\ x_1^2 & x_2^2 & \cdots & x_d^2 & | & f(X_2) \\ \vdots & \vdots & \ddots & \vdots & | & \vdots \\ x_1^N & x_2^N & \cdots & x_d^N & | & f(X_N) \end{bmatrix}.$$

The TLBO algorithm emulates the phase of teaching and learning from each other in a class, which improves the learners' academic performance.

4.2. ITLBO Algorithm

Considering the effect of temperature rise on motor parameters, an improved TLBO algorithm is investigated on the basis of offline identification data under the temperature rise conditions. Through an off-line identification experiment and by extending the temperature range to 0-100°, the upper and lower limit data can be obtained by off-line parameter identification, which is shown in Table 1.

Table 1. Parameter constraints of lower and upper values.

Parameter	Lower value	Upper value
R_s / mΩ	5.432	10.709
L_q / μH	28.942	39.731
L_d / μH	20.478	22.520
ψ_f / Wb	0.019	0.022

4.2.1. Initialization – ethnic migration

Compared to other intelligent algorithms, the TLBO requires fewer parameters, among which just the population size and the maximum iterations number need to be set. The initial population can be generated based on the following equation:

$$X_i = X_i^L + r \cdot \left(X_i^H - X_i^L \right), \tag{13}$$

where, X_i^H and X_i^L are the upper and lower limits of the decision variables, respectively. r is a random number in the range of $(0, 1)$.

The parameters of the hub motor will change with temperature rise.

By using the conventional TLBO identification method, the parameter drift caused by temperature change will make the population distribution wider, and affect its convergence speed and precision. The initialization program is improved according to the relationship between temperature and resistance. The corresponding subject of the stator resistance is initialized as follows:

$$X_i(1) = R_t + c \cdot \text{randn} \cdot D_i/2, \tag{14}$$

where $X_i(1)$ is the resistance corresponding to the student subject in the TLBO algorithm, R_t is the resistance value changing with the temperature t, D_i is the population distribution width,

Metrol. Meas. Syst., Vol. 30 (2023), No. 1, pp. 99–115
DOI: 10.24425/mms.2023.144396

which can be calculated by the error between the maximum resistance value $R_{\max}$ and the minimum value $R_{\min}t$ at the sampling temperature t, Randn is the normally distributed random number.

The Gaussian perturbation function can be used to initialize the cluster distribution and precisely follow the environment temperature while generating a small range of populations outside the defined range, which is shown in Fig. 1. This method can expand the search range pertinently and increase convergence accuracy. The probability distribution density of the initialized population in the range of D_i width is determined by the normal distribution coefficient$c$. The distribution density is 0.68 when $c = 1$ and the distribution density is 0.95 when $c = 0.5$. Fig. 2 and Fig. 3 show the schematic diagram of the initialized population distribution for resistance and magnet flux linkage at different temperatures, respectively. According to the previous analysis, the dq-axis inductances of the hub motor can be affected by many factors. The inductance changes of the dq-axis are nonlinear and not sensitive to the temperature. Therefore, the traditional TLBO algorithm is employed to initialize the $d-$axis and q-axis inductance of the hub motor. The initial population can be generated based on equation (15).

$$X(2,3) = X_{(2,3)}^{\min} + r \cdot \left(X_{(2,3)}^{\max} - X_{(2,3)}^{\min} \right). \tag{15}$$

A schematic diagram of the initialized population distribution for dq-axis inductances at different temperatures is shown in Fig. 4.

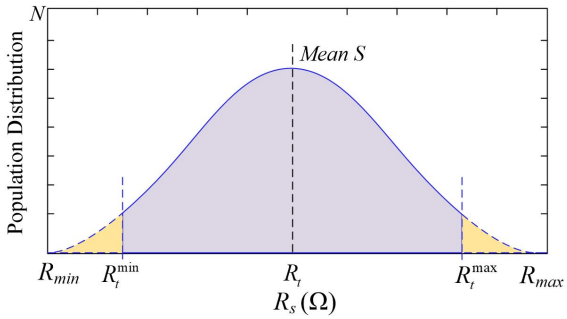

Fig. 1. Probability distribution of population initialization.

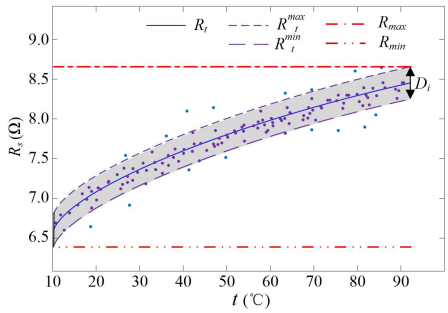

Fig. 2. Distribution of Rs initialization.

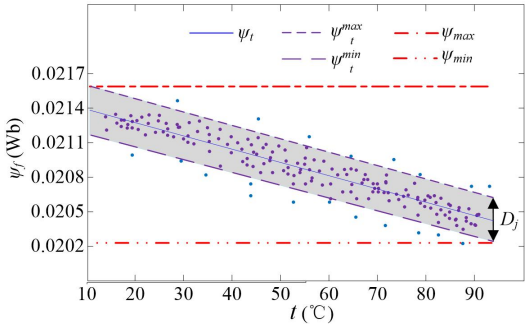

Fig. 3. Distribution of ψf initialization.

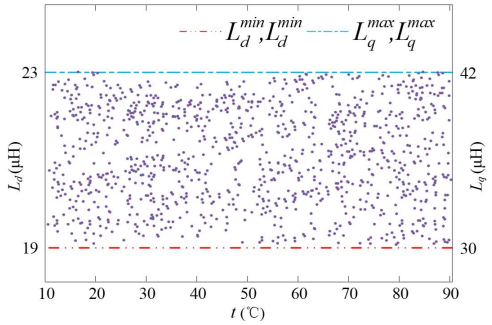

Fig. 4. Distribution of Ld and Lq initialization.

4.2.2. Teaching phase – teaching according to aptitude

The teacher strives to improve the average score of the class, and each student makes different progress. Many factors should be considered in the process of teaching, such as learning step size, teaching factor, and so on. The mathematical expressions of the teaching phase are shown in equations (16)–(17):

$$X_{\text{new},i} = X_i + r_i \cdot (X_T - TF \cdot \text{Mean}), \tag{16}$$

$$TF = \text{round}(1 + r), \tag{17}$$

$$\text{Mean} = \frac{1}{N}\sum_{1}^{N} X_i, \tag{18}$$

where, X_i and $X_{\text{new},i}$ denote the achievement of the i-th student before and after the study, respectively, Mean is the average achievement, r_i represents the learning step, TF is the teaching factor. The teaching quality is determined together by r_i and TF.

In this paper, a sinusoidal function is introduced to realize the teaching process, which is shown as equation (19). It is supposed to achieve rapid convergence to the global solution around the optimal solution.

$$X_{\text{new},i} = X_i + \sin(0.5\pi \cdot r_i) \cdot (X_T - TF \cdot \text{Mean}). \tag{19}$$

To better improve the overall performance of the class, the teacher will randomly select some students for individual tutoring after teaching, and teach students based on the differences between teachers and students.

$$X_{\text{new},j} = X_j + r_j \cdot (X_T - X_j). \tag{20}$$

Combining (19) and (20), and introducing the guidance factor p, which indicates the probability of being individually tutored by the teacher, namely the proportion of being tutored to the total number of people). The teaching phase can be expressed as shown in equation (21):

$$\begin{cases} X_{\text{new},i} = X_i + \sin(0.5\pi \cdot r_i) \cdot (X_T - TF \cdot \text{Mean}) + TP \cdot r_j \cdot (X_T - X_j) \\ TP = 1 \quad \text{rand} \le p \\ TP = 0 \quad \text{otherwise} \end{cases}. \tag{21}$$

4.2.3. Learning phase – group learning

The students also can learn from each other to improve their performance. Student X_i randomly selects another student X_j ($j \neq i$) as the learning object in the class. Equation (22) is used to describe the learning process:

$$\begin{cases} X_{\text{new},i} = X_i + r_i \cdot (X_i - X_j) & f(X_i) < f(X_j) \\ X_{\text{new},i} = X_i + r_i \cdot (X_j - X_i) & f(X_i) > f(X_j) \end{cases}. \tag{22}$$

The traditional TLBO learning mechanism consists in a student randomly looking for another student to study, but there is no guarantee that the students selected have better performances. In this paper, the group learning mechanism is adopted. All the students are divided into several groups and the top performers in each group are selected as team leaders. Firstly, the team leaders use traditional learning methods to learn from each other and improve their performance, in which the learning process is expressed as equation (23). Then, all team members compare their

Metrol. Meas. Syst., Vol. 30 (2023), No. 1, pp. 99–115
DOI: 10.24425/mms.2023.144396

knowledge with the team leader to learn the difference between each other and improve their results when the team leaders finish their learning. Finally, the groups are disbanded after each learning process, and the members are re-grouped during the next iteration. This solution can increase the communication learning path and avoid premature convergence.

$$X^g_{\text{new},i} = X^g_c + r_g \cdot \left(X^g_c - X^g_i\right), \tag{23}$$

where, X^g_c is the leader of the g group, X^g_i is the i-th member of group g.

The number of groups should be the factor of the number of students to ensure the average number of students in each group.

4.2.4. Low ranking elimination mechanism

The law of nature is survival of the fittest. The enterprises need to absorb fresh blood for performance, and the classes also need to absorb advanced students to improve results. This approach is inhumane in reality, but effective in algorithms. All students are ranked after each round of learning. The laggards are eliminated and new members are added, that is to say, the decision variables of the last β members are reassigned according to the initialization process. The low-ranking elimination mechanism not only improves the competitiveness to achieve the goal of rapid convergence, but also maintains the population width, prevents premature convergence, and improves the identification accuracy. At this stage, equation (13) is used to initialize the replacement parameters. That is because the addition of new parameters is used to ensure population diversity and avoid premature convergence, a larger range of spatial search is helpful to ensure the accuracy of identification.

4.3. Algorithmic Complexity Analysis

Let the number of iterations be t, population size be n. The tasks of the algorithm are mainly described in Step 2) and Step 3) in section 4.2 above. Time complexity for both steps is $O(n)$, then time complexity is $O(t \times n)$, spatial complexity is $O(n)$. The computational burden is mainly dependent on the iteration number and the population size of the algorithm.

4.4. Parameter Identification for Hub Motor Based on ITLBO Algorithm

4.4.1. Parameter Identification Principle and Mathematical Model for Hub motor

Parameter identification can be considered as the system search optimization strategy. u_d, u_q, i_d, i_q, and ω_e are the input variables of the parameter identification system. The control strategy of $i_d = 0$ is adopted in the hub motor drive system, which can be obtained by substituting in equation (3). The discretization of the voltage equation is described as:

$$\begin{cases} u_d(k) = -\omega_e(k) L_q i_q(k) \\ u_q(k) = R_s i_q(k) + L_q p i_q + \omega_e(k)_{fd} \end{cases}. \tag{24}$$

The rank of equation (24) is 2, for which the solution of four unknown quantities cannot be carried out. A full rank equation group is needed to satisfy the online identification of the parameters of R_s, L_d, L_q, and ψ_f. It is an effective way to realize full rank identification of parameters by increasing the disturbance signal to obtain a new identification equation [36]. The

short-time pulse current is injected into the negative direction of the d-axis. The mathematical model of the full-rank $d-$axis and $q-$axis can be described as equation (25):

$$\begin{cases} u_{d0}(k) = -\omega_{e0}(k) L_q i_{q0}(k) \\ u_{q0}(k) = R_s i_{q0}(k) + L_q p i_{q0}(k) + \omega_{e0}(k)\psi_f \\ u_{d1}(k) = R_s i_{d1}(k) - \omega_{e1}(k) L_q i_{q1}(k) \\ u_{q1}(k) = R_s i_{q1}(k) + L_q p i_{q1}(k) + \omega_{e1}(k)[L_d i_{d1}(k) + \psi_f] \\ p i_{q0}(k) = \dfrac{i_{q0}(k) - i_{q0}(k-1)}{h} \\ p i_{q1}(k) = \dfrac{i_{q1}(k) - i_{q1}(k-1)}{h} \end{cases}, \tag{25}$$

where h is the sampling step. The variables and parameters with subscript '0' are obtained from the control mode at $i_d = 0$. The variables and parameters with subscript '1' are obtained from the control mode at $i_d \neq 0$.

The data sampling process is shown in Fig. 5. Assuming $\hat{\phi} = \{\hat{R}_s, \hat{L}_d, \hat{L}_q, \hat{\psi}_f)\}$ are the estimated values of the parameter vectors to be estimated. $\hat{y} = \{\hat{u}_{d0}(k), \hat{u}_{q0}(k), \hat{u}_{d1}(k), \hat{u}_{q1}(k)\}$ are the estimated values of the output vectors of the drive system.

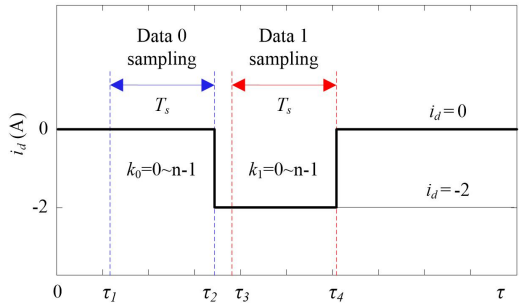

Fig. 5. Data sampling diagram.

According to equation (26), the TLBO algorithm equivalent tracking function is established as follows:

$$\begin{cases} \hat{u}_{d0}(k) = -\omega_{e0}(k)\hat{L}_q i_{q0}(k) \\ \hat{u}_{q0}(k) = \hat{R}_s i_{q0}(k) + \hat{L}_q p i_{q0}(k) + \omega_{e0}(k)\hat{\psi}_f \\ \hat{u}_{d1}(k) = \hat{R}_s i_{d1}(k) - \omega_{e1}(k)\hat{L}_q i_{q1}(k) \\ \hat{u}_{q1}(k) = \hat{R}_s i_{q1}(k) + \hat{L}_q p i_{q1}(k) + \omega_{e1}(k)[\hat{L}_d i_{d1}(k) + \hat{\psi}_f] \end{cases}. \tag{26}$$

A low-pass filter is employed to filter the voltage and current signal, and improve the identification accuracy.

Assuming a total of N sampling sessions is conducted in the sampling period T_s, the sampling data $\{y|y(0), y(1), \ldots, y(n-1)\}$ will be recorded as shown in Fig. 5. The fitness function of the TLBO algorithm is defined as follows:

$$F(\phi) = \sum_{k=1}^{n-1} \begin{bmatrix} w_1(u_{d0}(k) - \hat{u}_{d0}(k))^2 + w_2(u_{q0}(k) - \hat{u}_{q0}(k))^2 \\ +w_3(u_{d1}(k) - \hat{u}_{d1}(k))^2 + w_4(u_{q1}(k) - \hat{u}_{q1}(k))^2 \end{bmatrix}, \tag{27}$$

where, w_{1-4} are the weight factors, the values in this paper are 0.25.

Metrol. Meas. Syst., Vol. 30 (2023), No. 1, pp. 99–115
DOI: 10.24425/mms.2023.144396

4.4.2. Process of hub motor parameter identification based on the ITLBO algorithm

Fig. 6 shows the principle diagram of online multi-parameter identification based on the proposed ITLBO optimization algorithm for the hub motor.

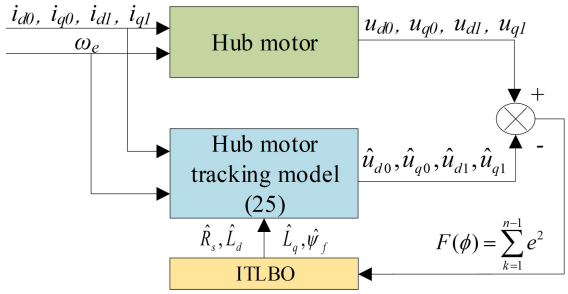

Fig. 6. Diagram of hub motor parameter identification based on ITLBO optimization algorithm.

5. Experiment and analysis of results

5.1. Experimental scheme and platform

The test platform of the hub motor shown in Fig. 7 is built for the verification of the proposed ITLBO method. Table 2 shows the specific parameters of the hub motor. Fig. 7 indicates the diagram of the experiment, including the drive circuit, the control circuit, and the identification algorithm. When the test platform is running, the control circuit commands the drive circuit to drive the hub motor and the magnetic powder brake is used as a load. The hub motor works with a constant speed of 350 r/min and a constant load of 50 Nm, during which the temperature of the stator of the hub motor rises from 20° to 80°. In addition, the control circuit also records the three-phase current, two-phase line voltage, hub motor speed, hub motor torque, and stator temperature of the hub motor with a real-time LMS data acquisition system with a sampling period of 100 μs and continuously uploads them to the computer. Finally, parameter identification results at different temperatures are obtained using the ITBLO identification algorithm designed in MATLAB.

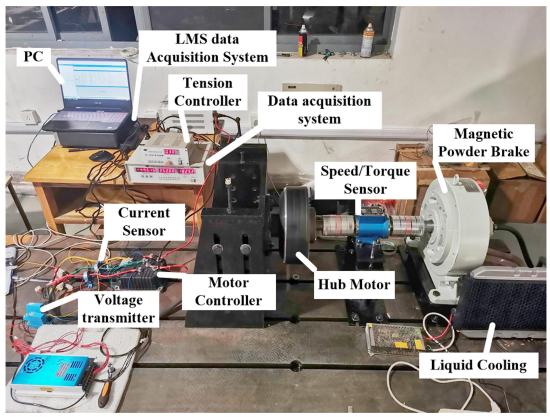

Fig. 7. Experimental platform for parameter identification of hub motor.

Table 2. Hub motor parameters.

Parameters	Value
Rated power (P / kW)	8.0
Rated Speed / (r/min)	1300
Rated voltage (U_n / V)	96
Rated Current (I_n / A)	50
Stator resistance (R_s / mΩ)	7.289 (30°)
d-axis inductance (L_d / μH)	20.623 (30°)
q-axis inductance (L_q / μH)	36.089 (30°)
Magnetic flux linkage (ψ_f / Wb)	0.0212 (30°)
Moment of inertia (J / kg·m^2)	0.168
Polar logarithm (N_p)	16

5.2. Experimental Results and their Analysis

The comparison results of parameter values and errors identified by the ITLBO algorithm, TLBO algorithm, IABC algorithm, and ABC algorithm under 350 r/min and 50 Nm conditions are presented in Fig. 8. E-ITLBO, E-TLBO, E-IABC, and E-ABC represent the identification errors of the ITLBO, TLBO, IABC, and ABC algorithms, respectively. As shown in Fig. 8a, the R_s values identified by the ITLBO, TLBO, IABC, and ABC algorithms increase with the temperature rise, respectively. That is consistent with the measured values at different temperatures identified by the offline identification method in Section 3. The absolute error of R_s identified by the TLBO and ABC algorithms is much larger than that of the ITLBO and IABC algorithms from 20° to 80°. Compared with the IABC algorithm, the ITLBO algorithm has the smallest identification error. From Fig. 8a, we can see the identified value of R_s is almost equal to the off-line identified value, which approximates 1% with the ITLBO algorithm and 2.2% with the IABC algorithm from 20° to 80°. That indicates that the proposed ITLBO algorithm has more robustness than the TLBO, IABC, and ABC algorithms. While the error of value obtained by the TLBO algorithm changes from 5% at 20°C to 7% at 80°C, and the error of value obtained by the ABC algorithm changes from 8% to 13%.

Fig. 8b shows that the values of L_d identified by the ITLBO, TLBO, IABC, and ABC algorithms increase smoothly with the temperature rise. The absolute error of L_d identified by the TLBO algorithm is about 5% below 50°C and about 6% when the temperature is more than 50°C. The absolute value error of L_d obtained by the ABC algorithm changes from 8.3% at 20°C to 12.8% at 80°C. The accuracy of results of the ITLBO and the IABC identification algorithm is higher within the range of test temperatures from 20°C to 80°C. From Fig. 8c, we can see L_q increases with the temperature rise. Fig. 8c also indicates that the absolute error of identification value of L_q obtained by the ITLBO algorithm is within 2%, and that generated by the IABC algorithm is within 5%. The TLBO algorithm has the largest identification error of approximately 4.5% at 60°C, and the smallest of approximately 3.8% at 20°C. The ABC algorithm has the largest identification error of approximately 10.6% at 80°C, and the smallest of approximately 7.5% at 30°C. Fig. 8d indicates the estimation result of flux linkage ψ_f. We can see the identification error of the ITLBO, TLBO, IABC, and ABC algorithms decrease with the temperature rise. The identification error of ψ_f obtained by the ITLBO algorithm is much smaller than that of the other algorithms.

Metrol. Meas. Syst., Vol. 30 (2023), No. 1, pp. 99–115
DOI: 10.24425/mms.2023.144396

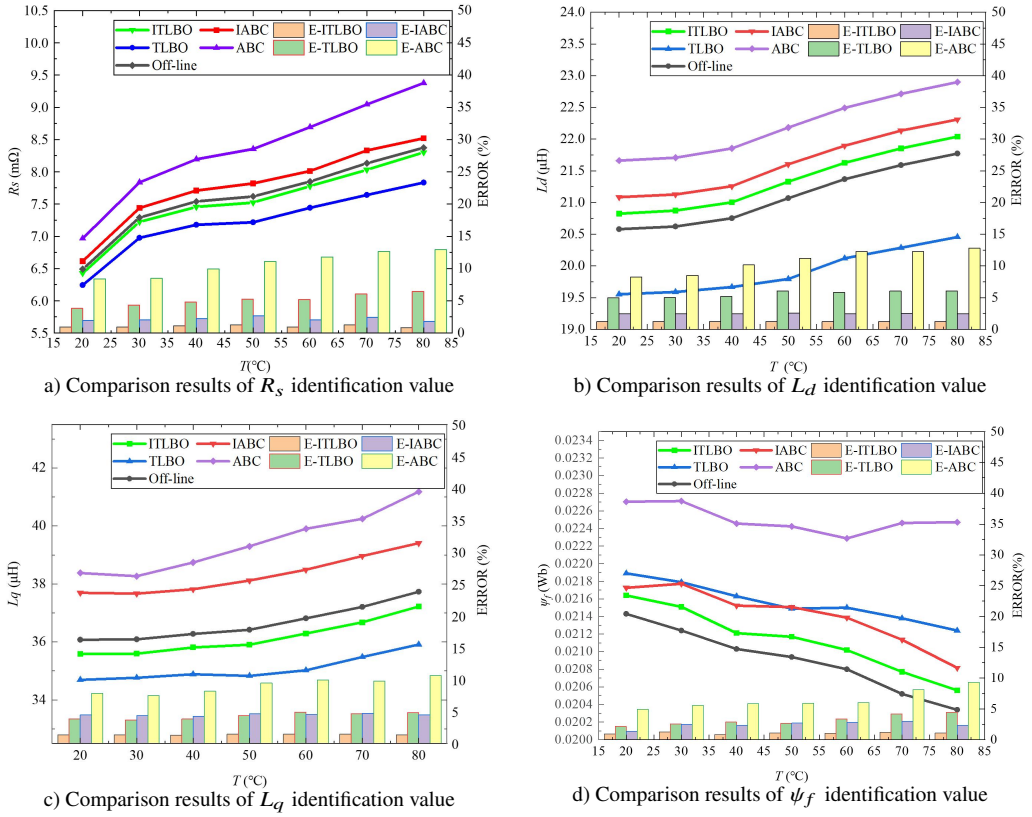

a) Comparison results of R_s identification value

b) Comparison results of L_d identification value

c) Comparison results of L_q identification value

d) Comparison results of ψ_f identification value

Fig. 8. Comparison of identification results identified by the different algorithms.

From the identification results we can see that the proposed ITLBO identification algorithm has higher identification accuracy and robustness from 20° to 80° than the TLBO, IABC, and ABC algorithms, which indicates the ITLBO algorithm can adapt well to the temperature rise. Moreover, the absolute error of the identification values hardly changes with temperature. The four parameters of the hub motor are coupled with each other, and the identification error of one parameter will affect the identification accuracy of the others. The identification accuracy of R_s and ψ_f can be improved directly by the proposed ITILBO algorithm at the optimized initialization phase. And, the identification accuracy of L_d and L_q can also be improved indirectly. The robustness of the ITLBO is effectively verified by experimental results.

6. Conclusions

Inspired by the traditional TLBO algorithm, the ITLBO algorithm for the hub motor is investigated in this paper, which accurately estimates the stator resistance, dq-axis inductances, and flux linkage with respect to temperature rise. The conclusions are listed as follows.

1. The temperature rise of the hub motor leads to complex nonlinear parameter variates under harsh operating conditions, especially for the conditions of frequent start, fast acceleration,

over-load torque and large current operation for a long time. The relationship between temperature and the offline value of R_s, L_d, L_q and ψ_f is analysed and modelled.

2. The ITLBO identification method is investigated to estimate the multi-parameter of the hub motor. The Gauss perturbation function is adopted to improve the initialization process. The group learning mechanism is employed to avoid the premature phenomenon. The 'rank test' is carried out when each teaching round completes. The last elimination mechanism is adopted to maintain population diversity, which effectively improves the identification speed and accuracy. The hub motor parameters that failed to be trained in the default cycle number are eliminated and replaced with newly initialized generated parameters.
3. The proposed ITLBO algorithm can not only maintain population diversity, but also prevent premature convergence. Compared with other identification algorithms, the global search ability, convergence speed, accuracy, and robustness of the ITLBO algorithm is improved, which has been verified by both of simulation and experimental results at different temperatures from 20° to 80°. The proposed ITLBO algorithm can adapt well to the temperature rise of the hub motor drive system in DDEVs.

Besides the temperature, magnetic saturation and VSI nonlinearities also lead to parameter drift, which poses great challenges to online parameter identification of the hub motor when it is operating in harsh conditions. Future work will focus on the online parameter identification caused by coupling of temperature rise, magnetic saturation, and VSI nonlinearities under long-time and overload operating conditions.

Acknowledgements

This work was supported by the National Natural Science Foundation of China (Grant No. 51705213), the China Postdoctoral Science Foundation (Grant No. 2019M660105 and Grant No. 2020T130360) and the Jiangsu Province Postdoctoral Science Foundation (Grant No. 2021K443C).

References

[1] Sun, X., Hu, C., Lei, G., & Yang, Z., & Zhu, J. (2020). Speed sensorless control of SPMSM drives for EVs with a binary search algorithm-based phase-locked loop. *IEEE Transactions on Vehicular Technology*, *69*(5), 4968–4978. https://doi.org/10.1109/TVT.2020.2981422

[2] L, S. Q., Ding, X. M., & Yu, B. (2022). Optimal control strategy of efficiency for dual motor coupling drive system of pure electric vehicle. *Journal of Jiangsu University (Natural Science Edition)*, *43*(1), 1–7.

[3] Li, Y., Zhang, B., & Xu, X. (2018). Robust control for permanent magnet in-wheel motor in electric vehicles using adaptive fuzzy neural network with inverse system decoupling. *Transactions of the Canadian Society for Mechanical Engineering*, *42*(3), 286–297. https://doi.org/10.1139/tcsme-2018-0027

[4] Liu, D., Wang, J., & Wang, S. (2022). Coordinated motion control and event-based obstacle-crossing for four wheel-leg independent motor-driven robotic system. *Mechatronics*, *81*, 102697. https://doi.org/10.1016/j.mechatronics.2021.102697

[5] Li, Y., Wu, H., & Zhang, B. H. (20) Frontier techniques and prospect of in-wheel motor for electric vehicle. *Journal of Jiangsu University (Natural Science Edition), 40*(03), 261–268.

[6] Besançon, G., Voda, A., & Popescu, A. (2022). Closed-loop-based observer approach for tunneling current parameter estimation in an experimental STM. *Mechatronics*, *83*, 102743. https://doi.org/10.1016/j.mechatronics.2022.102743

Metrol. Meas. Syst., Vol. 30 (2023), No. 1, pp. 99–115
DOI: 10.24425/mms.2023.144396

[7] Jiang, H., Zhou, Y., Xue, H. T., & Li, Z. X. (2021). Sequential diagnosis method for bearing fault of in-wheel motor based on CDI and AHNs. *Journal of Jiangsu University (Natural Science Edition), 42*(01), 15–21.

[8] Tang, X., Yang K., Wang, H., Wu, J., Qin, Y., Yu, W., & Cao, D. (2022). Prediction-Uncertainty-Aware Decision-Making for Autonomous Vehicles. *IEEE Transactions on Intelligent Vehicles*, *7*(4), 849–862. https://doi.org/10.1109/TIV.2022.3188662

[9] Mahmud, M. H., Wu, Y., & Zhao, Y. (2020). Extremum Seeking-Based Optimum Reference Flux Searching for Direct Torque Control of Interior Permanent Magnet Synchronous Motors. *IEEE Transactions on Transportation Electrification*, *6*(1), 41–51. https://doi.org/10.1109/TTE.2019.2962327

[10] Tang X., Chen, J., Liu, T., Qin, Y., & Cao D. (2021). Distributed Deep Reinforcement Learning-Based Energy and Emission Management Strategy for Hybrid Electric Vehicles. *IEEE Transactions on Vehicular Technology*, *70*(10), 9922–9934. https://doi.org/10.1109/TVT.2021.3107734

[11] Li, H., Zhang, X., Xu, C., & Hong, J. (2020). Sensorless Control of IPMSM Using Moving-Average-Filter Based PLL on HF Pulsating Signal Injection Method. *IEEE Transactions on Energy Conversion*, *35*(1), 43–52. https://doi.org/10.1109/TEC.2019.2946888

[12] Zhao, W., Yang, A., Ji, J., Chen, Q., & Zhu, J. (2019). Modified Flux Linkage Observer for Sensorless Direct Thrust Force Control of Linear Vernier Permanent Magnet Motor. *IEEE Transactions on Power Electronics*, *34*(8), 7800–7811. https://doi.org/10.1109/TPEL.2018.2879411

[13] Li, Y., Huang, Y., & Xu, X. (2019). A novel hybrid control approach for modular automation system: a case study of sensorless interior permanent magnet in-wheel motor. *Assembly Automation*, *39*(5), 840–853. https://doi.org/10.1108/AA-08-2018-0120

[14] Bašić, M., Vukadinović, D., Grgić, I., & Bubalo, M. (2020). Speed-Sensorless Vector Control of an Induction Generator Including Stray Load and Iron Losses and Online Parameter Tuning. *IEEE Transactions on Energy Conversion*, *35*(2), 724–732. https://doi.org/10.1109/TEC.2019.2952666

[15] Yuan, C.C., Zhang, H.F., He, Y.G., Shen, J., & Chen, L. (2022). Identification of adhesion coefficient ahead based on image feature and HMM. *Journal of Jiangsu University (Natural Science Edition)*, *43*(04), 373–380.

[16] Fang, J., & Han, B. (2018). High-Precision Parameter Identification of High-Speed Magnetic Suspension Motor. *IEEE Transactions on Energy Conversion*, *33*(1), 20–31. https://doi.org/10.1109/TEC.2016.2620802

[17] Yang, C., Bu, L., & Chen, B. (2021). Energy modeling and online parameter identification for permanent magnet synchronous motor driven belt conveyors. *Measurement*, *178*, 109342. https://doi.org/10.1016/j.measurement.2021.109342

[18] Rafaq, M. S., Mwasilu, F., Kim, J., Choi, H. H., & Jung, J. W. (2017). Online Parameter Identification for Model-Based Sensorless Control of Interior Permanent Magnet Synchronous Machine. *IEEE Transactions on Power Electronics*, *32*(6), 4631–4643. https://doi.org/10.1109/TPEL.2016.2598731

[19] Yao, Y., Huang, Y., Peng, F., & Dong, J. (2020). Position Sensorless Drive and Online Parameter Estimation for Surface-Mounted PMSMs Based on Adaptive Full-State Feedback Control. *IEEE Transactions on Power Electronics*, *35*(7), 7341–7355. https://doi.org/10.1109/TPEL.2019.2957058

[20] Wang, Y., Xu, Y., & Zou, J. (2020). Online Multiparameter Identification Method for Sensorless Control of SPMSM. *IEEE Transactions on Power Electronics*, *35*(10), 10601–10613. https://doi.org/10.1109/TPEL.2020.2974870

[21] Wang, Q., Wang, G., Zhao, N., Zhang, G., Cui, Q., & Xu, D. (2021). An Impedance Model-Based Multiparameter Identification Method of PMSM for Both Offline and Online Conditions. *IEEE Transactions on Power Electronics*, *36*(1), 727–738. https://doi.org/10.1109/TPEL.2020.3000896

[22] Liu, Z. H., Wei, H. L., Zhong, Q. C., Liu, K., Xiao, X. S., & Wu, L. H. (2017). Parameter Estimation for VSI-Fed PMSM Based on a Dynamic PSO with Learning Strategies. *IEEE Transactions on Power Electronics*, *32*(4), 3154–3165. https://doi.org/10.1109/TPEL.2016.2572186

[23] Liu, K., & Zhu, Z. Q. (2015). Quantum Genetic Algorithm-Based Parameter Estimation of PMSM under Variable Speed Control Accounting for System Identifiability and VSI Nonlinearity. *IEEE Transactions on Industrial Electronics*, *62*(4), 2363–2371. https://doi.org/10.1109/TIE.2014.2351774

[24] Pan, Y., Sun, T., & Yu, H. (2019). On parameter convergence in least squares identification and adaptive control. *International Journal of Robust and Nonlinear Control*, *29*(10), 2898–2911. https://doi.org/10.1002/rnc.4527

[25] Zerdali, E. (2020). A Comparative Study on Adaptive EKF Observers for State and Parameter Estimation of Induction Motor. *IEEE Transactions on Energy Conversion*, *35*(3), 1443–1452. https://doi.org/10.1109/TEC.2020.2979850

[26] Zhang, L. W., Zhang, P., Liu, Y. F., Zhang, C., & Liu, J. (2018). Parameter identification of permanent magnet synchronous motor based on variable step-size Adaline neural network. *Transactions of China Electrotechnical Society*, *33*(S2), 377–384. https://doi.org/10.19595/j.cnki.1000-6753.tces.L80266 (in Chinese)

[27] Xiao, X., Xu, Q., Wang, Y., & Shi, Y. (2014). Parameter identification of interior permanent magnet synchronous motors based on genetic algorithm. *Transactions of China Electrotechnical Society*, *29*(3), 21–26.

[28] Cao, Y., Zhang, H., Li, W., Zhou, M., Zhang, Y., & Chaovalitwongse, W. A. (2018). Comprehensive learning particle swarm optimization algorithm with local search for multimodal functions. *IEEE Transactions on Evolutionary Computation*, *23*(4), 718–731. https://doi.org/10.1109/TEVC.2018.2885075

[29] Guo-han, L., Jing, Z., Zhao-hua, L., & Kui-yin, Z. (2015). Parameter identification of PMSM using improved comprehensive learning particle swarm optimization. *Electric Machines and Control*, *19*(1), 51–57. https://doi.org/10.15938/j.emc.2015.01.008 (in Chinese)

[30] Zhang, J. C., Wang, T., Wang, L. M., Zou, X. J., & Song, W. (2021). Optimization control strategy of driving torque for slope-crossing of pure electric vehicles. *Journal of Jiangsu University (Natural Science Edition)*, *42*(05), 506–512.

[31] Haghdar, K. (2019). Optimal DC source influence on selective harmonic elimination in multilevel inverters using teaching–learning-based optimization. *IEEE Transactions on Industrial Electronics, 67*(2), 942–949. https://doi.org/10.1109/TIE.2019.2901657

[32] Zhou, Y., Huang, K., Sun, P., & Dong, R. (2020). Analytical Calculation of Performance of Line-Start Permanent-Magnet Synchronous Motors Based on Multidamping-Circuit Model. *IEEE Transactions on Power Electronics, 36*(4), 4410–4419. https://doi.org/10.1109/TPEL.2020.3025172

[33] Li, Y., Wu, H., Xu, X., Cai, Y., & Sun, X. (2019). Analysis on electromechanical coupling vibration characteristics of in-wheel motor in electric vehicles considering air gap eccentricity. *Bulletin of the Polish Academy of Sciences. Technical Sciences*, *67*(5). https://doi.org/10.24425/bpasts.2019.130882

[34] Liu, J.Y., Bi, S., Wu, D. H., & Yang, Z.G. (2021). Sensitivity analysis of parameters for controllable transformer rectifier. *Journal of Jiangsu University (Natural Science Edition), 42*(04), 466–472.

Metrol. Meas. Syst., Vol. 30 (2023), No. 1, pp. 99–115
DOI: 10.24425/mms.2023.144396

[35] Accetta, A., Alonge, F., Cirrincione, M., D'Ippolito, F., Pucci, M., & Sferlazza, A. (2020). GA-Based Off-Line Parameter Estimation of the Induction Motor Model Including Magnetic Saturation and Iron Losses. *IEEE Open Journal of Industry Applications, 1*, 135–147. https://doi.org/10.1109/OJIA.2020.3024567

[36] Liu, K., Zhang, Q., Chen, J., Zhu, Z. Q., & Zhang, J. (2010). Online multiparameter estimation of nonsalient-pole PM synchronous machines with temperature variation tracking. *IEEE Transactions on Industrial Electronics, 58*(5), 1776–1788. https://doi.org/10.1109/TIE.2010.2054055

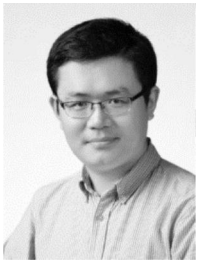

Yong Li is currently an associate professor with the Automotive Engineering Research Institute, Jiangsu University, China. He once studied at the University of Waterloo, Ontario, Canada. He has published more than 30 papers. His research interests include motor control and drive, vehicle system dynamics, complex electromechanical coupling systems.

Taohua Zhang received the Master Degree in vehicle engineering from the University of Science and Technology Beijing, Beijing, China, in 2011. He is currently a senior engineer with Beijing Institute of Space Launch Technology, Beijing, China. His research interests include overall technology of launch equipment based on electric drive system.

Han Hu received the B.Sc. degree in vehicle engineering from Huaiyin Institute of Technology, Huaian, Jiangsu Province, China, in 2020. He is currently working toward the master's degree in vehicle engineering at Jiangsu University, Zhenjiang, China. His current research interests include motor parameter identification and sensorless control.

Juan Wang received her M.Sc. in vehicle engineering from the University of Science and Technology Beijing, Beijing, China, in 2011. She is currently an engineer with Beijing Institute of Space Launch Technology, Beijing, China. Her research interests include overall technology of launch equipment based on electric drive systems.

Hao Wu received the B.Sc. degree in vehicle engineering from Huaiyin Institute of Technology, Huaian, Jiangsu Province, China, in 2018 and M.S. degree in vehicle engineering with Jiangsu University, Zhenjiang, Jiangsu Province, China, in 2021. His current research interests include motor parameter identification and sensorless control.